High-Throughput Proteomic-Based Identification of Oxidatively Induced Protein Carbonylation in Mouse Brain

Brian A. Soreghan,[1] Frank Yang,[2] Stefani N. Thomas,[1] Jennifer Hsu,[1] and Austin J. Yang[1,3]

Received March 10, 2003; accepted August 6, 2003

Purpose. The major initiative of this study was to implement a novel proteomic approach in order to detect protein carbonylation in aged mouse brain. Several lines of evidence indicate that reactive oxygen species (ROS)-induced protein oxidation plays an essential role in the initiation of age-related neuropathologies. Therefore, the identification of free radical or peroxide substrates would provide further insight into key biochemical mechanisms that contribute to the progression of certain neurological disorders.

Methods. Historically, ROS targets have been identified by conventional immunological two-dimensional (2-D) gel electrophoresis and mass spectrometric analyses. However, specific classes of proteins, such as transmembrane-spanning proteins, high-molecular-weight proteins, and very acidic or basic proteins, are frequently excluded or underrepresented by these analyses. In order to fill this technologic gap, we have used a functional proteomics approach using a liquid chromatography tandem mass spectrometric (LC-MS/MS) analysis coupled with a hydrazide biotin-streptavidin methodology in order to identify protein carbonylation in aged mice.

Results. Our initial studies suggest an ability to identify at least 100 carbonylated proteins in a single LC-MS/MS experiment. In addition to high-abundance cytosolic proteins that have been previously identified by 2-D gel electrophoresis and mass spectrometric analyses, we are able to identify several low-abundance receptor proteins, mitochondrial proteins involved in glucose and energy metabolism, as well as a series of receptors and tyrosine phosphatases known to be associated with insulin and insulin-like growth factor metabolism and cell-signaling pathways.

Conclusions. Here we describe a rapid and sensitive proteomic analysis for the identification of carbonylated proteins in mouse brain homogenates through the conjunction of liquid chromatography and tandem mass spectrometry methods. We believe the ability to detect these post-translationally modified proteins specifically associated with brain impairments during the course of aging should allow one to more closely and objectively monitor the efficacy of various clinical treatments. In addition, the discovery of these unique brain biomarkers could also provide a conceptual framework for the future design of alternative drugs in the treatment of a variety of age-related neurodegenerative disorders.

KEY WORDS: proteomic analysis; carbonylated proteins; aging; mouse; brain.

INTRODUCTION

The generation of free radicals and the degree to which they cause oxidative injury play important roles in the process of aging and various age-related degenerative diseases. The free radical theory of aging suggests that irreversible, deleterious changes of biological systems are primarily caused by increased oxidative damage to key macromolecules such as DNA, proteins, and lipids by free radicals (1,2).

Currently, it is widely accepted that protein oxidation and reactive oxygen species (ROS) generation are tightly linked to a series of pathological processes during the course of age-related neurologic disorders and that the oxidative modification of certain key molecules is sufficient to initiate select pathological events (3–6). Protein carbonylation content is widely used as a marker to determine the level of protein oxidation that is caused either by the direct oxidation of amino acid side chains (e.g., proline and arginine to γ-glutamylsemialdehyde, lysine to aminoadipic semialdehyde, and threonine to aminoketobutyrate) or via indirect reactions with oxidative by-products [lipid peroxidation derivatives such as 4-hydroxynonenal (HNE) (Fig. 1), malondialdehyde (MDA), and advanced glycation end products (AGEs)] (2,4). A deleterious consequence of these oxidative impairments is protein dysfunction. For instance, a recent report indicates that HNE causes a direct inactivation of lysosomal cathepsin B activity *in vitro* (7). Mass spectrometric analysis of HNE-conjugated cathepsin B suggests that a loss of cathepsin B enzymatic activity is directly attributed to HNE adduction of His^{150} and Cys^{290} within the active site of the protein (7). In addition, Keller and co-workers report the detrimental effects of lipid peroxidation on neuronal plasticity (8). Isolated synaptosomes treated with HNE evoke mitochondrial disruption and impairment of glutamate transport. Although the specific molecular mechanisms leading to these alterations remain largely unclear, biochemical studies suggest that there is a direct correlation between the adduction of HNE to a glutamate transporter and loss of glutamate transporter function (8).

Numerous studies also demonstrated that there is a direct correlation among increased levels of protein carbonylation, progression of aging, and cognitive decline (9–11). For example, markers of protein carbonylation can be detected in both senile plaques and paired-helical filament (PHF-1)-positive tangles, further supporting the notion that oxidative modifications play a pivotal role in Alzheimer's disease (AD) pathogenicity. Although increased protein carbonylation in AD has been reported for many years, the detailed pathologic significance of such oxidative modifications has remained largely unknown. By using a combination of Oxyblot and two-dimensional (2-D) gel electrophoresis, Aksenova and coworkers have found that the levels of oxidative modification of β-actin and creatine kinase BB are higher in AD than in control brains. In addition, the carbonylation of both β-actin and creatine kinase BB is observed earlier than neurofibrillary degeneration in neurons of AD, further strengthening the theory that age-related oxidative stress could be a primary risk factor involved in the initial stages of AD pathogenesis (12). A similar proteomics approach using 2-D gel electrophoresis coupled with mass spectrometric analysis has also been used to identify potential biologic targets of protein carbonylation in AD (13). These investigators have identified several proteins, such as dihydropyrimidinase-related protein-2 (DRP-2), α-enolase, and heat shock cognate 71 (HSC-71), that are post-translationally modified by lipid peroxidation. However, one should also note that only select proteins show increases in the levels of carbonylation in AD. For ex-

[1] Department of Pharmaceutical Sciences, University of Southern California School of Pharmacy, Los Angeles, California 90089.
[2] Micro-Tech Scientific, Inc., 2330 Cousteau Court, Vista, CA 92083-8346.
[3] To whom correspondence should be addressed. (email: austiny@usc.edu)

0724-8741/03/1100-1713/0 © 2003 Plenum Publishing Corporation

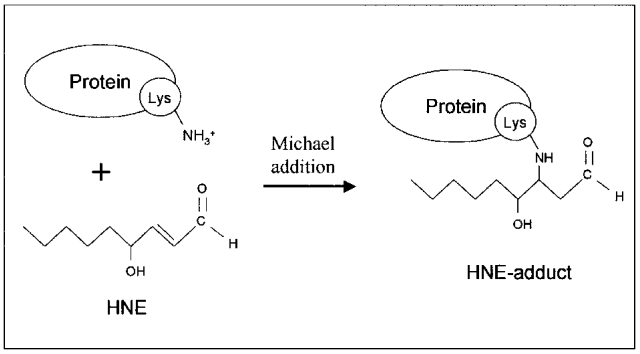

Fig. 1. Schematic diagram of carbonylation of amino acid side chains by free aldehydes. 4-Hydroxynonenal (HNE) is an example of a reactive aldehyde that can be produced through the oxidation of unsaturated fatty acids such as arachidonic and linoleic acids. HNE can introduce aldehyde groups into a protein by forming Michael adducts with the side chains of histidine, lysine and/or cysteine residues. The adduction of HNE to a lysine residue on a protein is represented here.

ample, HSC-71 and β-tubulin are known to be carbonylated in AD, but there are no detectable differences in carbonylation levels of these two proteins between normal age-matched controls and AD cases. As a consequence, Butterfield *et al.* have suggested that only certain proteins in AD brain are vulnerable to ROS-mediated modifications (13).

Toward our goal of understanding the effects of post-translational modifications of proteins during the course of aging and neurodegeneration, we report a sensitive detection method for the occurrence of protein carbonylation in aged mice through the use of a newly developed shotgun proteomic approach known as multiple-dimensional protein identification technology (MudPIT) (14). Traditional proteomic analyses are accomplished through the implementation of 2-D gel electrophoresis (to separate and visualize proteins) in tandem with mass spectrometry (for protein identification). Although these technologies have been widely used in the field of proteomics, it is well known that 2-D gel electrophoresis/mass spectrometric analysis can reliably detect only high-abundance proteins (15). In addition, the potential for protein comigration within a given spot further limits the use of 2-D gel electrophoresis as a tool for proteomic analysis. Here we describe a rapid and sensitive alternative for the identification of carbonylated proteins in mouse brain homogenates through the conjunction of a liquid chromatography and tandem mass spectrometry method. By using these technologies, we have been able to identify ~100 different carbonylated proteins in a single experiment. Furthermore, this method has also allowed us to detect several different classes of proteins, such as those of the transmembrane, large-molecular-weight, and low-abundance varieties, which are traditionally difficult to detect by 2-D gel electrophoresis alone.

MATERIALS AND METHODS

Tissue Homogenization

Approximately 50–100 mg of brain tissue from 3-week- and 18-month-old C57B mice (four and eight animals, respectively) was cut into small pieces on dry ice and subsequently homogenized with a hand-held tissue disruptor in lysis buffer [50 mM sodium acetate (pH 5.5), 150 mM NaCl, 1% Triton X-100, 0.1% SDS, 1 mM EDTA] containing a protease inhibitor cocktail with AEBSF, aprotinin, leupeptin, bestatin, pepstatin A, and E-64 (Sigma product P8340). Samples were centrifuged at 18,000 × *g* for 30 min at 4°C. Supernatants were separated from the pellets and subsequently reacted with the hydrazide reagent.

Protein Carbonyl Labeling, Affinity Purification, and Tryptic Digestion

Aliquots of 300 μl of 5 mM EZ-Link™ biocytin hydrazide (Pierce product 28020) dissolved in 100 mM sodium acetate (pH 5.5) were added to 600 μl of each of the supernatants. The samples were incubated for 1 h at room temperature, and 200 μl of 100 mM Tris (pH 7.5) was added to each tube to stop the reaction. Sodium cyanoborohydride was added to a final concentration of 10 mM in order to stabilize the reaction products. Then, 100 μl of ImmunoPure-immobilized streptavidin (Pierce product 20347) was added to each sample, and samples were rotated overnight at 4°C. After centrifugation and transfer of the supernatant, the agarose beads containing the bound protein were washed twice with lysis buffer and twice with 100 mM ammonium bicarbonate (pH 8.5). After 400 μl of 100 mM ammonium bicarbonate (pH 8.5) was added to each tube, samples were subsequently reduced with DTT and alkylated with iodoacetamide. The samples were then centrifuged again, and following removal of the supernatant, ammonium bicarbonate was again added, and samples were treated with 0.5 μg of trypsin (Sigma product T-1426, TPCK-treated). The digestion reactions were incubated by rotation at 37°C for 2 h. This method was repeated an additional two times, and the final incubation was 16 h. After trypsin treatment, samples were centrifuged, and the supernatants containing tryptic fragments were collected and subsequently lyophilized until analysis by mass spectrometry.

Mass Spectrometry

All samples were analyzed using a Finnigan LCQ Classic ion trap mass spectrometer (Thermo Finnigan, San Jose, CA). One-dimensional liquid chromatography was conducted with an Ultra Plus II Proteomic System (Micro-Tech Scientific, Inc., Vista, CA) equipped with 15cm × 75μm (ID) reverse-phase (RP) capillary columns (in-tube end frits packed with 5μm C18, 300Å particles) from Micro-Tech Scientific. Samples were loaded onto a RP column with 99% mobile phase solvent A (5% acetonitrile, 1% formic acid) and 1% solvent B (95% acetonitrile, 0.8% formic acid). Peptides were eluted with a linear gradient of 1–95% solvent B for 100 min. The mass spectrometer was equipped with an LCQ nanospray ion source (Thermo Finnigan) and 10μm (ID) noncoated SilicaTip™ PicoTip™ nanospray emitters (New Objective, Woburn, MA). The electrical contact was made through a liquid junction at the PEEK union. The spray voltage of the mass spectrometer was set to 1.5 kV, and the heated capillary temperature to 160°C.

MS/MS Data Generation and Analysis

Tandem MS/MS spectra were acquired with Xcalibur 1.2 software using the following method: a full MS scan was followed by three consecutive MS2 scans of the top three ion peaks from the preceding full scan using dynamic exclusion

(four repetitions in 1.5 min were excluded for 3 min). Data were analyzed using Bioworks 3.1, Beta-test site version from Thermo Finnigan, utilizing the SEQUEST algorithm to determine cross-correlation scores between acquired spectra and a mouse protein database. The following parameters were used for the TurboSEQUEST search analyses: no enzyme was chosen for the protease because not all proteins are digested to completion, molecular weight range 400–4500, threshold 1000, monoisotopic, precursor mass 1.4, group scan 10, minimum ion count 20, charge state auto, peptide 1.5, fragment ions 0, and differential amino acid modifications Cys 57.0520. Results were filtered using SEQUEST cross-correlation scores greater than 1.5 for +1 ions, 2.0 for +2 ions, and 2.5 for +3 ions.

RESULTS

Accumulating evidence suggests that elevated levels of carbonylated proteins serve as a seminal biochemical alteration in the course of aging and various neurological disorders. To further our investigations of aging and neurodegeneration with respect to protein modifications, we have developed a new method for detecting and identifying carbonylated proteins utilizing a shotgun proteomics approach in combination with an affinity purification method that enriches for these modified proteins and is shown schematically in Fig. 2.

Identification of Carbonylated Proteins by Tandem Mass Spectrometry and SEQUEST Algorithm

A conventional liquid chromatography mass spectrometric analysis initially involves the separation of peptide fragments by a reverse-phase (RP) column to resolve peptide fragments by hydrophobicity. Peptide fragments are eluted directly into the ion source of a tandem mass spectrometer, which isolates and induces fragmentation of these peptides, resulting in a mass spectrum of the fragment ions for each peptide that is recorded. A computer algorithm, SEQUEST, is used to match the acquired tandem mass spectra with theoretical spectra generated from a sequence database to identify peptide sequences within the protein mixture. By using the SEQUEST algorithm, peptides with molecular masses matching that of the parent peptide ion from the tandem mass spectrometer are extracted from a protein database. The top 500 matching peptides are then subjected to a more extensive ion-matching algorithm in order to generate cross-correlation scores. Thus, a list of peptides with their corresponding correlation scores is produced, and protein identifications are evaluated based on these scores.

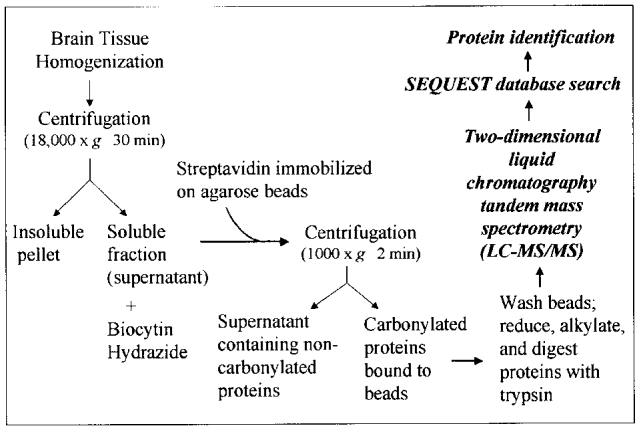

Fig. 2. Schematic representation of the identification of the carbonylated proteins from mouse brain homogenates generated by the implementation of a biocytin hydrazide–streptavidin affinity purification method in combination with a liquid chromatography tandem mass spectrometric proteomic approach.

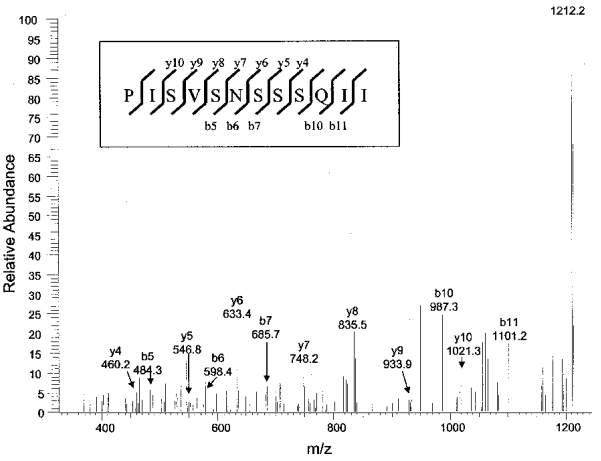

Fig. 3. Tandem mass spectrum of an insulin receptor peptide. Mass spectra generated from LC-MS/MS were subjected to a SEQUEST database search to match a theoretical MS/MS spectrum from a NCBI mouse protein TFASTA database.

Summary of Carbonylated Proteins from Aged Mice

Figure 3 demonstrates a typical peptide identification by LC-MS/MS analysis. A precursor ion is first isolated and then fragmented to form a product ion (MS/MS) spectrum. Because the location of peptide fragmentation along the backbone is predictable, SEQUEST software can be used to match a predicted tandem mass spectrum from a database with an acquired tandem mass spectrum. As indicated in Fig. 3, a peptide derived from the insulin receptor was sequenced (amino acid sequence: PISVSNSSSQII) and identified by this methodology. In this study, each raw tandem mass spectrum was processed as follows: (a) spectra derived from single or multiply charged parent ions were first identified; (b) the selected charged ions were then subjected to a final protein identification analysis through the SEQUEST algorithm using the following cross-correlation score parameters: >1.5 for +1 ions, 2.0 for +2 ions, and 2.5 for +3 ions. By using this method, we were able to identify over 100 proteins in a single run, hence allowing for a more comprehensive investigation of oxidative protein modifications.

Table I shows a partial list of proteins from a total of ~100 identified in one representative aged (18 months) mouse brain sample by this liquid chromatography mass spectrometric analysis. Table IA lists several cytoskeletal proteins including α- and β-tublin, β-actin, and integrin. Table IB includes a list of mitochondrial proteins that are known to be involved in both redox regulation and ATP generation. Table IC consists of a group of cell-signaling regulatory proteins, including several proteins and receptors that are tightly associated with insulin and the insulin-like growth factor signal transduction pathway as well as phosphatases involved in controlling the phosphorylation state of numerous key signaling proteins.

Table I. Identification of Carbonylated Proteins in Aged Mice by LC-MS/MS and SEQUEST

No.	Peptide	m/z	Charge	Xcorr
A. Cytoskeletal/structural proteins				
1.	(NM_006087) tubulin, beta, 5			
	R.EIVHLQAGQC*GNQIGAK.F	1822.95	3	2.58
	R.FPGQLNADLR.K	1130.60	2	2.82
	R.SGPFGQIFRPDNFVFGQSGAGNNWAK.G	2798.34	2	4.03
	R.SGPFGQIFRPDNFVFGQSGAGNNWAK.G	2798.34	2	2.62
2.	(NM_001101) beta actin; beta cytoskeletal actin			
	R.GYSFTTTAER.E	1132.53	2	2.68
	R.GYSFTTTAER.E	1132.53	2	2.29
	K.LC*YVALDFEQEMATAASSSSLEK.S	2550.20	2	2.80
3.	B25819 actin, fetal skeletal/adult cardiac muscle–mouse (fragment)			
	K.EITALAPSTMK.I	1161.62	1	2.22
	K.IWHHTFYNELR.V	1515.75	3	2.82
	K.EITALAPSTMK.I	1161.62	1	1.70
4.	(NM_017379) tubulin, alpha 8; tubulin alpha 8 [*Mus musculus*]			
	R.LDHKFDLMYAK.R	1380.70	3	3.80
	R.NLDIERPTYTNLNR.L	1718.88	2	2.10
5.	S53793 actin–mouse (fragments)			
	-.AVFPSIVGRPR.V	1198.71	2	2.28
	-.AVFPSIVGRPR.V	1198.71	2	2.81
6.	(NM_008319) intercellular adhesion molecule 5, telencephalin [*Mus musculus*]			
	N.LGLSSNNSTLSVAGAMGSHGGEYEC*AATNAH.G	3063.38	2	2.04
7.	(NM_021359) integrin beta 6 [*Mus musculus*]			
	I.ETNSSKCHNGNGSFQCGVCTCNPGHMGPHCEC*GEDM.V	3827.43	3	2.66
8.	A61189 tubulin beta chain–mouse (fragment) [*Homo sapiens*]			
	X.EIVHXQAGQC*GNQIGAK.F	1822.95	3	2.58
9.	(NM_023279) tubulin, beta 3 [*Mus musculus*]			
	R.EIVHIQAGQC*GNQIGAK.F	1822.95	3	2.58
10.	B25437 tubulin beta-2 chain–mouse (fragment)			
	K.EVDEQMLNVQNK.N	1446.69	1	2.40
11.	TBA2_MOUSE Tubulin alpha-2 chain (Alpha-tubulin 2)			
	K.DVNAAIATIK.T	1015.58	1	2.11
B. Redox regulation and energy metabolism				
1.	(NM_015804) ATPase, class 1, member h; ATPase 11A, p type; ATPase 11A,			
	F.MVLFNYIIPVSMYVTVEMQKF.L	2552.30	2	2.48
2.	(NM_010497) isocitrate dehydrogenase 1 ($NADP^+$), soluble [*Mus musculus*]			
	S.QFEAQNIC*YEHRLIDDMVAQA.M	2551.20	2	2.66
3.	SCB1_MOUSE Succinyl-CoA ligase [ADP-forming] beta-chain, mitochondrial precursor			
	K.INFDSNSAYR.Q	1186.55	2	2.26
4.	I49427 cytochrome P450 16a-ms1–western wild mouse			
	S.FNDENLLIVVRD.L	1446.76	1	2.34
5.	CP1B_MOUSE CYTOCHROME P450 1B1 (CYPIB1) (P450CMEF) (P450EF)			
	R.DMTDAFILSAEK.K	1340.64	3	2.57
6.	(XM_110106) similar to superoxide dismutase [Mn], mitochondrial precursor			
	G.SFEKFKEKLTAVSVGVQG.S	1954.07	1	1.50
C. Glucose metabolism and cell signaling regulatory proteins				
1.	(NM_019564) protease, serine, 11 (Igf binding); insulin-like growth factor			
	G.PC*GEGLQCVLPFGVPASATVRRRAQAGLC.V	3013.56	2	2.28
	G.PCGEGLQC*VLPFGVPASATVRRRAQAGLC.V	3013.56	2	2.19
	E.GPCGEGLQCVLPFGVPASATVRRRAQAGLC.V	3013.53	2	2.28
2.	(NM_010568) insulin receptor [*Mus musculus*]			
	H.CQKVCPTICKSHGCTAEGLCCHKECLGNCSEPDDPTKC*V.A	4196.79	3	2.66
	H.CQKVCPTICKSHGCTAEGLCCHKEC*LGNCSEPDDPTKCV.A	4196.79	3	2.64
	H.CQKVCPTICKSHGCTAEGLCCHKECLGNC*SEPDDPTKCV.A	4196.79	3	2.67
3.	A57293 latent transforming growth factor beta-binding protein 3 precursor–mouse			
	D.FPAACIGGDC*INTNGSYRC*LCPLGHRLVGGRKC*KK.D	3878.99	3	2.56
	D.FPAACIGGDC*INTNGSYRCLC*PLGHRLVGGRKC*KK.D	3878.99	3	2.70
4.	(NM_018766) neurotensin receptor [*Mus musculus*]			
	S.DLLILLLAMPVE.L	1339.79	3	2.92
	S.DLLILLLAMPVE.L	1339.79	3	2.59

Table I. Continued

No.	Peptide	m/z	Charge	Xcorr
5.	(NM_008984) protein tyrosine phosphatase, receptor-type, M [*Mus musculus*]			
	T.RC*HSYNLTVHYGYQVG.G	1953.93	1	1.54
6.	I73044 substance P, NK-1 receptor–mouse (fragment)			
	Y.HICVTVLIYFL.P	1320.74	1	1.52
7.	(NM_008976) protein tyrosine phosphatase, nonreceptor type 14 [*Mus musculus*]			
	G.HKLVSPSDQMNPQNCAMPIKPGAS.S	2550.23	2	2.43
8.	(NM_009706) Rho GTPase activating protein 5 [*Mus musculus*]			
	G.EIVETANTVAPQPTSNPG.Q	1824.90	1	2.04
9.	B30310 glucose transport protein GT2			
	D.DGEPPRQRVTGTLVLAVF.S	1955.07	1	1.53
10.	(NM_011210) protein tyrosine phosphatase, receptor type, C [*Mus musculus*]			
	T.CGPPYETNGPKTFYILVVRSGGSFVTNTTKTNCQF.Y	3826.86	3	2.89
11.	PN0020 fibroblast growth factor receptor 2–mouse			
	D.DVQSINWLR.D	1130.60	2	2.06
12.	S50893 protein-tyrosine-phosphatase (EC 3.1.3.48), receptor type sigma			
	M.EGAEARGAPRIKDIMLADAQEMVITN.L	2799.41	2	2.40

To attempt to qualitatively identify age-specific, oxidatively modified, carbonylated protein targets, we conducted the same biocytin hydrazide–streptavidin–LC-MS/MS analysis on brain tissue of 3-week-old mice to compare our results with those from our 18-month-old mouse samples. An abbreviated list of proteins compiled from both sets (aged vs. young mice) of experiments is shown in Table II, which is divided into three parts. These include carbonylated proteins identified (a) only in aged mice, (b) in both aged and young mice, and (c) only in young mice. For example, the α peptide of the q subcomponent of complement component 1, caspase 11, TNF member 8, and the acetylcholine receptor α subunit were identified in five, four, three, and two out of eight aged mice, respectively, but were not identified in any of the four young mice. We also found carbonylation targets that were identified only in young mice and not in aged mice. For example, LIM/homeobox protein Lhx8 and synapsin I were identified in four and three out of four young mice, respectively, but were not identified in any of the eight aged mice. However, the largest category was comprised of carbonylated proteins identified in both young and aged brain tissue, and these included the complement receptor type 2 precursor, semaphorin 4B, the low-density lipoprotein receptor, dynamin-1, and the tubulin α_2 chain (see Table II middle section).

DISCUSSION

In this report, we have developed a sensitive and high-throughput proteomic method to examine the protein targets of carbonylation in the brains of aged mice. Many reports indicate a strong link between aging and protein carbonylation. In particular, several carbonylated proteins have been successfully isolated by coupling Oxyblot and 2-D gel electrophoresis matrix-assisted time-of-flight mass spectrometry methods. However, certain types of proteins are often excluded or underrepresented in 2-D gel electrophoresis. These proteins include very basic, acidic, or transmembrane proteins. Furthermore, it is well documented that 2-D gel/mass spectrometric analysis is not capable of detecting low-abundance proteins without any pregel enrichment (16). As a result, we decided to institute an alternative approach to identify oxidative modification of proteins through a recently developed on-line microcapillary reverse-phase LC-MS/MS analysis. The integration of liquid column chromatography and tandem mass spectrometry provides several advantages over 2-D gel electrophoresis. The method is rapid and thus allows one to identify several hundred proteins in a complicated mixture within 2–3 days. In addition, peptide sequencing by tandem mass spectrometry can be accomplished by acquiring a single scan at sensitivities requiring only low-femtomole levels of proteins. Our initial studies suggest that over 100 carbonylated proteins can be identified by our LC-MS/MS method. Many of the proteins identified in this study can be divided into four different groups: those that are involved in cytoskeletal organization, mitochondrial energy metabolism, redox regulation, and signal transduction (see Table I). The degree to which any one of these proteins is rendered dysfunctional by a carbonyl modification and the extent to which they might act in a causal role toward the aging process or in neurodegenerative diseases is the subject of future and more elaborate investigations, but it is interesting to note that many proteins identified here have previously been identified in age-related disorders.

Oxidation of Cytoskeletal Proteins

Oxidative alterations of cytoskeletal proteins, such as β-tubulin and β-actin, have been recently identified in AD through immunohistochemical and 2-D gel electrophoresis analyses (17). In particular, the levels of cytoskeletal protein carbonylation were significantly increased in AD brains, suggesting a causal relationship between cytoskeletal changes and these oxidative impairments (17). Interestingly, several recent studies indicate that the presence of carbonyl formation on neurofibrillary tangles (NFT) may also play an important role in the formation of NFT during the course of Alzheimer's disease (18). Biochemical studies reveal that the modification of NFTs by HNE can lead to cross-linking and that this alteration is essential for the initial assembly of paired helical filaments (PHF) that comprise NFTs (18). Oxidation of tau protein *in vitro* has also been shown to cause tau insolubility, which is consistent with a model that suggests that adduction of tau by reactive aldehydes can stabilize PHF formation and ultimately lead to NFT development (18).

Table II. A Partial List of Carbonylated Proteins Identified in Aged and Young Mouse Brain Tissue by a Biocytin Hydrazide-Streptavidin Affinity–Tandem Mass Spectometric Approach

Protein	Aged mice (n = 8)	Young mice (n = 4)
A. Identified only in aged mice		
(NM_007572) complement component 1, q subcomponent, alpha polypeptide	5	0
(NM_007609) caspase 11 [*Mus musculus*]	4	0
(NM_013689) cytoplasmic tyrosine kinase, Dscr28C related (*Drosophila*) (Tec)	3	0
(NM_009137) chemokine (C-C motif) ligand 22 (Ccl22)	3	0
(NM_009403) tumor necrosis factor (ligand) superfamily, member 8 [*Mus musculus*]	3	0
(NM_008402) integrin alpha V; vitronectin receptor alpha polypeptide	3	0
(NM_028075) BAFF receptor [*Mus musculus*]	3	0
(XM_132371) G-protein coupled receptor 27 [*Mus musculus*]	3	0
(XM_130351) acetylcholine receptor alpha subunit [*Mus musculus*]	2	0
SM4F_MOUSE Semaphorin 4F precursor (Semaphorin W)	2	0
SCB1_MOUSE Succinyl-CoA ligase [ADP-forming] beta-chain, mitochondrial precursor	2	0
(NM_007444) S-Adenosylmethionine decarboxylase 2 [*Mus musculus*]	2	0
B. Identified in both aged and young mice		
(NM_009172) seven in absentia 1A (Siah1a) [*Mus musculus*]	4	1
(NM_013490) choline kinase; CK/EK-alpha; choline/ethanolamine kinase alpha	3	1
(NM_013643) protein tyrosine phosphatase, non-receptor type 5	2	1
CR2_MOUSE Complement receptor type 2 precursor (Cr2) (Complement C3d receptor)	2	1
(NM_011767) zinc finger RNA binding protein [*Mus musculus*]	2	1
(NM_011163) eukaryotic translation initiation factor 2 alpha kinase 2	1	1
(NM_008101) glucagon receptor [*Mus musculus*]	1	1
JG0193 G protein-coupled receptor FEX–mouse (*Drosophila*) [*Mus musculus*]	4	2
I48922 cation-independent mannose 6-phosphate/insulin-like growth factor II receptor	3	2
(NM_010568) insulin receptor [*Mus musculus*]	3	2
(NM_012035) transient receptor potential cation channel, subfamily C	3	2
LMA3_MOUSE Laminin alpha-3 chain precursor (Nicein alpha subunit)	3	2
LMG2_MOUSE Laminin gamma-2 chain precursor (Kalinin/nicein/epiligrin 100 kDa subunit)	3	2
(NM_011161) mitogen-activated protein kinase 11 (Mapk11)	3	2
SM4B_MOUSE Semaphorin 4B (Semaphorin C)	3	2
I48623 low density lipoprotein receptor–mouse	2	2
SUCA_MOUSE Succinyl-CoA ligase [GDP-forming] alpha-chain, mitochondrial precursor	2	2
(NM_023370) cadherin 23 (otocadherin) (Cdh23) [*Mus musculus*]	4	3
DYN1_MOUSE Dynamin-1 (Dynamin BREDNM19)	2	3
A1A4_MOUSE Sodium/potassium-transporting ATPase alpha-4 chain (Sodium pump 4)	2	3
(NM_008512) low density lipoprotein receptor-related protein 1	4	4
TBA2_MOUSE Tubulin alpha-2 chain (Alpha-tubulin 2)	4	4
C. Identified only in young mice		
(NM_023279) tubulin, beta 3 (Tubb3) [*Mus musculus*]	0	4
LHX8_MOUSE LIM/homeobox protein Lhx8	0	4
(NM_007505) ATP synthase, H+ transporting, mito. F1 complex, alpha sub., iso. 1 (Atp5a1)	0	3
(NM_011587) tyrosine kinase receptor 1 [*Mus musculus*]	0	3
(NM_007930) ectodermal-neural cortex 1 (Enc1) [*Mus musculus*]	0	3
(NM_013680) synapsin 1 [*Mus musculus*]	0	3
SCB2_MOUSE Succinyl-CoA ligase [GDP-forming] beta-chain, mitochondrial precursor	0	2

Oxidative Damage and Mitochondrial Dysfunction

Another noteworthy observation in our results is the number of mitochondrial proteins (as well as cytochrome P450) affected by oxidative impairment (Table IB). Mitochondria are the major sites of ROS generation and oxidative damage; the accumulation of oxidized proteins within the mitochondrion has been suggested as a key factor in age-related processes. Changes in mitochondrial redox potential have also been linked to various physiologic processes including ATP synthesis, cell death initiation, and regulation of respiratory functions. However, the physiologic targets of ROS in mitochondria are largely unknown. Of the five carbonylated mitochondrial proteins listed in Table IB (ATPase, isocitrate dehydrogenase, succinyl-CoA ligase, cytochrome P450, and superoxide dismutase), the first three are involved in ATP production, and thus, it is possible that structural alteration of one or all of these proteins would have detrimental effects on normal mitochondrial function and ATP metabolism. Interestingly, cytochrome P450 and superoxide dismutase (SOD), which are known to be centrally involved in the detoxification of ROS within the mitochondrion, are also subjected to carbonylation. Although it is not clear whether the adduction of carbonyl groups on either superoxide dismutase or cytochrome P450 could alter the functions of these proteins, it is known that SOD ablation in *Sod* (–/–) mice results in a lethal

phenotype within the first week of life (19–21). The identification of SOD and cytochrome P450 as carbonylated substrates in this study also provides the first biochemical evidence supporting a direct correlation between declining mitochondrial function and increased ROS production in the mitochondrion during the course of aging.

Alteration of the Phosphatase/Kinase Balance in Aged Mice

Interestingly, several proteins involved in signal transduction and cell signaling have also been identified as ROS targets. For example, several reports indicate that insulin resistance is known to play a critical role in type 2 diabetes mellitus. In addition, senile individuals affected by CNS diseases, such as Alzheimer's disease and Parkinson's disease, are prone to insulin resistance and type 2 diabetes mellitus and related hypoglycemia (a risk factor for stroke). Although the molecular mechanisms leading to the alterations of insulin-signaling pathways in the CNS remain elusive, a recent report indicates a direct correlation between decreased expression of sulfhydryl-containing tyrosine phosphatase 2 and down-regulation of insulin-response elements in aged animals (22). Our study agrees with this report in that we also identify carbonylated tyrosine phosphatases in aged mice. Interestingly, a recent investigation by Lu *et al*. indicates that the lipid peroxidation product HNE can modulate gating of voltage-dependent Ca^{2+} channels in neurons through up-regulation of protein tyrosine phosphorylation (23). Although the molecular mechanisms that cause increased protein tyrosine phosphorylation in HNE-treated neurons are currently unclear, our results suggest that this increase in tyrosine phosphorylation could be explained, at least in part, by an alteration of tyrosine phosphatase activity by protein carbonylation.

Alterations in the balance of protein kinase/phosphatase activities have been shown to parallel reduced synaptic responses during aging (24). For instance, treatment of brain slices established from aged animals with the phosphatase inhibitor calyculin A causes an increase in synaptic response. These data suggest a shift in the kinase/phosphatase balance during aging. Hence, enzymes involved in phosphorylation/dephosphorylation do clearly play an essential role in the maintenance of neuronal plasticity (24). A recent report by Genoux and co-workers suggests that protein phosphatase 1 (PP1) plays a crucial role in the efficacy of learning and memory by limiting acquisition and favoring memory decline (25). For example, when PP1 is blocked during learning exercises, shorter intervals between training episodes are sufficient for optimal performance in younger animals. Moreover, blockage of PP1 activity prevents memory decline (forgetting) in aged animals (25). One possible explanation for these disturbances in the kinase/phosphatase balance may be amino acid side chain oxidation of key phosphatases.

A Need for Quantitative Proteome Profiling

In this initial study, we were able to qualitatively identify carbonylated proteins in both aged and young mouse brain tissue, suggesting that even in very young (3-week-old) animals, proteins can undergo carbonylation. Some of these identified proteins were represented only in aged or only in young mice, but the majority of carbonylated protein targets were found to be present in members of both groups (Table II). The ability to determine which modified proteins may be predominantly found in aged mice requires an extensive statistical analysis and the need for quantification.

One major limitation of our current method and most mass spectrometric-based protein identification methods has been the inability to attain global quantitative proteome profiling. However, several emerging technologies have shown significant progress toward this goal by combining stable isotope protein labeling, multidimensional chromatography, tandem mass spectrometry, and automated database searches. One of the most commonly used techniques to label and quantify proteins utilizes isotope-coded affinity tag (ICAT) reagents (26). These ICAT-labeled proteins are identified by a LC-MS/MS method similar to the one we describe here. However, the relative abundances of these labeled proteins are subsequently calculated based on peak intensity ratios of isotope pairs of peptide ions detected by the tandem mass spectrometer. As a result, the identification and quantification of peptides can be measured "on-the-fly" and determined simultaneously. Although this ICAT-based methodology can be highly automated, the mass spectrometer can consume a significant amount of time detecting proteins that are highly abundant, that are constitutively expressed, and/or that have very little clinical or biologic significance. Therefore, it is has been suggested that it may be more advantageous to uncouple the peptide identification and quantification technologies and that quantification should precede peptide identification. A recent study incorporating this methodology has demonstrated a dramatic advance in quantitative proteomic analysis, and as a consequence, this new approach allows users to be more selective in identifying those proteins that have a more pertinent role in biologic and clinical problems (27).

Practical Considerations for Protein Identification from Mass Spectrometry Data

One should also note that cabonylated proteins represent only a fraction of the total amount of oxidatively modified proteins. For instance, histidine, tryptophan, methionine, and phenylalanine can be oxidized into other modified amino acids (e.g., histidine to oxohistidine and aspartate, tryptophan to kynurenines, methionine to methionine sulfoxide, and phenylalanine to *ortho*- and *meta*-tyrosine (1,28). As a consequence, these types of modifications would not be identified by our biocytin-hydrazide-streptavidin affinity purification and mass spectrometric approach. Another point worthy of mention is that there is a general concern of nonspecific binding of noncarbonylated proteins to streptavidin-agarose beads. Although we can not completely rule out this possibility at this point, most carbonylated proteins identified in Table IIA–C are in general agreement with carbonylated proteins identified by previous DNP-based Oxyblot/2-D gel mass spectrometric analysis or anti-HNE antibody studies (8,12,13). Currently, we are in the process of identifying the sites of carbonylation by various tandem mass spectrometric and bioinformatics approaches to further confirm our studies directly. Finally, it should be noted that most proteins identified in this report are largely based on a single MS/MS spectrum per protein; thus, the identification of each protein will need to be verified manually rather than identified solely through a database search. This issue becomes more critical if the protein is part of large gene family. For example, our data

clearly indicate that β-actin is present in our affinity-purified carbonylated protein samples, but it is known that β-actin belongs to a large, highly conserved gene family. Consequently, it is not possible to distinguish the origins of a single peptide if this peptide sequence is located within some highly conserved domain of the actin gene family. The identification of a specific actin protein will require the presence of a gene-specific peptide in order to be positively identified by tandem mass spectrometry.

In summary, we believe that the identification of proteins directly isolated via a liquid chromatography tandem mass spectrometric approach provides many significant advantages over a conventional 2-D gel electrophoresis/mass spectrometric analysis. In addition, a liquid chromatography method can potentially be modified into a more highly automated 2-D system, allowing one to process more complicated samples. In fact, a rapid and highly sensitive 2-D chromatography tandem mass spectrometric method has been recently described (14). As a result, more than 12,000 unique peptides can be resolved by this type of approach, and it was possible to identify ~1600 unique proteins in a single experiment. In conclusion, the results presented in this report indicate our ability to identify multiple proteins as free radical targets, and further biochemical characterization of these proteins should allow us to gain further insight into the roles of free radical damage and the pathophysiologic consequences of protein oxidation during the course of aging and the development of some age-related neurologic disorders.

ACKNOWLEDGMENTS

This work was supported by a grant awarded by the National Institutes of Health (A.Y., MH59786) as well as an Alzheimer's Association award (A.Y.). We express our special thanks to Dr. Tina Tekirian, Dr. David Tabb, Brad Hart, and Amy Zumwalt for their technical assistance and critical discussions concerning the content of this manuscript.

REFERENCES

1. E. R. Stadtman. Protein oxidation in aging and age-related diseases. *Ann. N. Y. Acad. Sci.* **928**:22–38 (2001).
2. E. Shacter. Quantification and significance of protein oxidation in biological samples. *Drug Metab. Rev.* **32**:307–326 (2000).
3. M. J. Picklo, T. J. Montine, V. Amarnath, and M. D. Neely. Carbonyl toxicology and Alzheimer's disease. *Toxicol. Appl. Pharmacol.* **184**:187–197 (2002).
4. Y. H. Wei and H. C. Lee. Oxidative stress, mitochondrial DNA mutation, and impairment of antioxidant enzymes in aging. *Exp. Biol. Med.* **227**:671–682 (2002).
5. M. A. Korolainen, G. Goldsteins, I. Alafuzoff, J. Koistinaho, and T. Pirttila. Proteomic analysis of protein oxidation in Alzheimer's disease brain. *Electrophoresis* **23**:3428–3433 (2002).
6. G. Perry, A. Nunomura, K. Hirai, X. Zhu, M. Prez, J. Avila, R. J. Castellani, C. S. Atwood, G. Aliev, L. M. Sayre, A. Takeda, and M. A. Smith. Is oxidative damage the fundamental pathogenic mechanism of Alzheimer's and other neurodegenerative diseases? *Free Radic. Biol. Med.* **33**:1475–1479 (2002).
7. J. W. Crabb, J. O'Neil, M. Miyagi, K. West, and H. F. Hoff. Hydroxynonenal inactivates cathepsin B by forming Michael adducts with active site residues. *Protein Sci.* **11**:831–840 (2002).
8. J. N. Keller, R. J. Mark, A. J. Bruce, E. Blanc, J. D. Rothstein, K. Uchida, G. Waeg, and M. P. Mattson. 4-Hydroxynonenal, an aldehydic product of membrane lipid peroxidation, impairs glutamate transport and mitochondrial function in synaptosomes. *Neuroscience* **80**:685–696 (1997).
9. D. A. Butterfield and J. Kanski. Brain protein oxidation in age-related neurodegenerative disorders that are associated with aggregated proteins. *Mech. Ageing Dev.* **122**:945–962 (2001).
10. D. A. Butterfield, A. Castegna, C. M. Lauderback, and J. Drake. Evidence that amyloid beta-peptide-induced lipid peroxidation and its sequelae in Alzheimer's disease brain contribute to neuronal death. *Neurobiol. Aging* **23**:655–664 (2002).
11. D. A. Butterfield and C. M. Lauderback. Lipid peroxidation and protein oxidation in Alzheimer's disease brain: potential causes and consequences involving amyloid beta-peptide-associated free radical oxidative stress. *Free Radic. Biol. Med.* **32**:1050–1060 (2002).
12. M. V. Aksenova, M. Y. Aksenov, R. M. Payne, J. Q. Trojanowski, M. L. Schmidt, J. M. Carney, D. A. Butterfield, and W. R. Markesbery. Oxidation of cytosolic proteins and expression of creatine kinase BB in frontal lobe in different neurodegenerative disorders. *Dement. Geriatr. Cogn. Disord.* **10**:158–165 (1999).
13. A. Castegna, M. Aksenov, V. Thongboonkerd, J. B. Klein, W. M. Pierce, R. Booze, W. R. Markesbery, and D. A. Butterfield. Proteomic identification of oxidatively modified proteins in Alzheimer's disease brain. Part II: dihydropyrimidinase-related protein 2, alpha-enolase and heat shock cognate 71. *J. Neurochem.* **82**:1524–1532 (2002).
14. M. P. Washburn, D. Wolters, and J. R. Yates III. Large-scale analysis of the yeast proteome by multidimensional protein identification technology. *Nat. Biotechnol.* **19**:242–247 (2001).
15. S. P. Gygi, G. L. Corthals, Y. Zhang, Y. Rochon, and R. Aebersold. Evaluation of two-dimensional gel electrophoresis-based proteome analysis technology. *Proc. Natl. Acad. Sci. USA* **97**:9390–9395 (2000).
16. J. Peng and S. P. Gygi. Proteomics: the move to mixtures. *J. Mass Spectrom.* **36**:1083–1091 (2001).
17. M. Y. Aksenov, M. V. Aksenova, D. A. Butterfield, J. W. Geddes, and W. R. Markesbery. Protein oxidation in the brain in Alzheimer's disease. *Neuroscience* **103**:373–383 (2001).
18. T. Wataya, A. Nunomura, M. A. Smith, S. L. Siedlak, P. L. Harris, S. Shimohama, L. I. Szweda, M. A. Kaminski, J. Avila, D. L. Price, D. W. Cleveland, L. M. Sayre, and G. Perry. High molecular weight neurofilament proteins are physiological substrates of adduction by the lipid peroxidation product hydroxynonenal. *J. Biol. Chem.* **277**:4644–4648 (2002).
19. S. Melov, P. E. Coskun, and D. C. Wallace. Mouse models of mitochondrial disease, oxidative stress, and senescence. *Mutat. Res.* **434**:233–242 (1999).
20. L. A. Esposito, S. Melov, A. Panov, B. A. Cottrell, and D. C. Wallace. Mitochondrial disease in mouse results in increased oxidative stress. *Proc. Natl. Acad. Sci. USA* **96**:4820–4825 (1999).
21. S. Melov, P. Coskun, M. Patel, R. Tuinstra, B. Cottrell, A. S. Jun, T. H. Zastawny, M. Dizdaroglu, S. I. Goodman, T. T. Huang, H. Miziorko, C. J. Epstein, and D. C. Wallace. Mitochondrial disease in superoxide dismutase 2 mutant mice. *Proc. Natl. Acad. Sci. USA* **96**:846–851 (1999).
22. M. H. Lima, M. Ueno, A. C. Thirone, E. M. Rocha, C. R. Carvalho, and M. J. Saad. Regulation of IRS-1/SHP2 interaction and AKT phosphorylation in animal models of insulin resistance. *Endocrine* **18**:1–12 (2002).
23. C. Lu, S. L. Chan, W. Fu, and M. P. Mattson. The lipid peroxidation product 4-hydroxynonenal facilitates opening of voltage-dependent Ca^{2+} channels in neurons by increasing protein tyrosine phosphorylation. *J. Biol. Chem.* **277**:24368–24375 (2002).
24. C. M. Norris, S. Halpain, and T. C. Foster. Alterations in the balance of protein kinase/phosphatase activities parallel reduced synaptic strength during aging. *J. Neurophysiol.* **80**:1567–1570 (1998).
25. D. Genoux, U. Haditsch, M. Knobloch, A. Michalon, D. Storm, and I. M. Mansuy. Protein phosphatase 1 is a molecular constraint on learning and memory. *Nature* **418**:970–975 (2002).
26. S. P. Gygi, B. Rist, S. A. Gerber, F. Turecek, M. H. Gelb, and R. Aebersold. Quantitative analysis of complex protein mixtures using isotope-coded affinity tags. *Nature Biotechnol.* **10**:994–999 (1999).
27. T. J. Griffin, C. M. Lock, X. J. Li, A. Patel, I. Chervetsova, H. Lee, M. E. Wright, J. A. Ranish, S. S. Chen, and R. Aebersold. Abundance ratio-dependent proteomic analysis by mass spectrometry. *Anal. Chem.* **75**:867–874 (2003).
28. J. R. Requena, C. C. Chao, R. L. Levine, and E. R. Stadtman. Glutamic and aminoadipic semialdehydes are the main carbonyl products of metal-catalyzed oxidation of proteins. *Proc. Natl. Acad. Sci. USA* **98**:69–74 (2001).